RESEARCH AND DEVELOPMENT OF DOUBLE TETRAHEDRON HEXA-ROTORCRAFT (DOT-HR)

Daichi TORATANI*
***Graduate School of Environment and Information Sciences, Yokohama National University**
toratani-daichi-yn@ynu.ac.jp

Keywords: *UAV design, Multi-rotor, Attitude control, Free flight experiment*

Abstract

The automatic flight of the multi-rotorcrafts is one of the hot topics of unmanned aerial vehicle systems. This paper is on development of newly designed rotorcraft called double tetrahedron Hexa-Rotorcraft. The new rotorcraft has unique configuration and characteristic that the rotorcraft does not have to incline its attitude when the vehicle is moving in horizontal direction.

In this paper, the motion performance of the dot-HR is demonstrated by the free flight experiment using the experimental testbed. The experimental testbed is built with several elements, for example, inertial measurement unit, attitude controller and navigation controller. Before the free flight experiment, these elements are tested their performance. From these results, the free flight experiment is held, and finally the unique ability of the dot-HR is confirmed

Nomenclature

ϕ, θ, ψ: Euler angle of rotorcraft [deg]
p, q, r: angular velocity $[deg/s]$
α: elevation angle of thrust [deg]
F_x, F_y, F_z: force acting on body [N]
M_ϕ, M_θ, M_ψ: torque acting on body $[N \cdot m]$
T_i: thrust of rotor i $(i = 1, 2, \cdots 6)$ [N]
l: edge length of tetrahedron [m]
acc_x, acc_y: acceleration measured by accelerometer $[m/s^2]$
g: acceleration of gravity $[m/s^2]$
I_x, I_y, I_z: inertial moment $[kg \cdot m^2]$
Q: gain matrix of LQR

1 Introduction

The automatic flight of the unmanned aerial vehicles (UAVs) is one of the hot topics in aeronautics. UAVs are able to be divided into fixed and rotary wing type. The different types of the wings give different type of characteristics for the vehicle such as payload, stabilization, surveillance, and etc... Amongst all, the multi-rotors have high payload and high stabilization. So-called quad-rotors as shown in Figure 1 are used to demonstrate the ability of the rotorcraft as future UAV system [1-6]. Compared to single-rotorcrafts, the multi-rotorcrafts have extra redundancy, extra payload, simple configuration, and higher stability for various missions. These characteristics make multi-rotorcrafts a feasible system for UAVs.

The unmanned surveillance of isolated indoor is currently one of the greatest interest in Japan due to the Fukushima nuclear plant accident. Currently, a lot of navigation systems adapt global positioning system (GPS) [7, 8], but GPS is not able to obtain accurate position indoors. So, there is no system that

Fig. 1 Photo of quadrotor (STARMAC) [1]

is able to fly in indoor environment without having any information about the surrounding environment. To achieve the unmanned surveillance for indoor, feasible collision avoidance system is needed for safer flight. Laser range sensor is one of the sensors studied widely for collision avoidance in uncertain environment [9-12]. However, this sensor is not able to scan accurate data with tilting, and traditional rotorcrafts must incline its attitude to move in horizontal direction.

In Yokohama National University, the hexa-rotorcraft with non-plane configuration is currently under development for automatic indoor surveillance of isolated environment. The rotorcraft has 6 rotors at the edge of tetrahedrons placed in opposite of each other as shown in Figure 2. This rotorcraft is named double tetrahedron Hexa-Rotorcraft (dot-HR) from its unique configuration. The dot-HR has advantage that the vehicle does not need to incline when it is moving in horizontal direction where all of other rotorcrafts have to tilt its attitude toward the heading direction. This will enable the rotorcraft to have easier system for visionary sensing, easier environment information monitoring by the laser range sensors and easier stabilization control for the vehicle is able to move around in its stabilized condition. These advantages are very large when the vehicle is moving in isolated area.

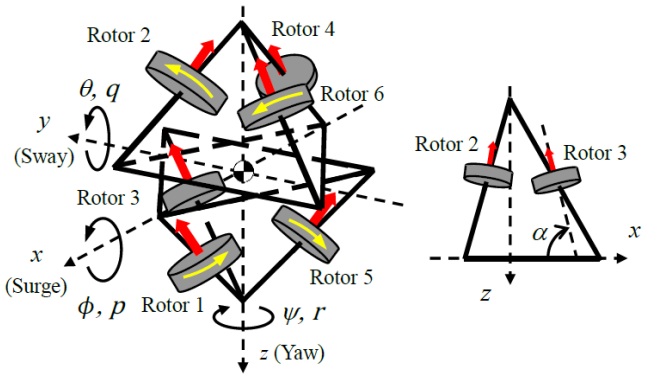

Fig. 2 Construction of dot-HR

2 Double Tetrahedron Hexa-Rotorcraft

2. 1 Mathematical Model

Figure 2 shows the multi-rotor used in this study. This multi-rotor has 2 tetrahedrons placed in opposite of each other. The rotors are arranged at the one third of the edges of the tetrahedrons with elevation angle α. So the rotors are placed in 3-dimensional arrangement. In this study, the α is 75 [deg], and the edge length of the tetrahedron is 0.6 [m] derived by the numerical optimization. The rotors on the top 3 rotate in counter-clockwise and rotors on the bottom 3 rotate in clockwise direction, which eliminates the effect of anti-torques. Equation 1 shows the equation of motion of the rotorcraft.

$$f = Au \tag{1}$$

Here, f, A and u are

$$f^T = (F_x \quad F_y \quad F_z \quad M_\phi \quad M_\theta \quad M_\psi) \tag{2}$$

$$A = \begin{pmatrix} \cos\alpha & -\frac{1}{2}\cos\alpha & -\frac{1}{2}\cos\alpha & \cos\alpha & -\frac{1}{2}\cos\alpha & -\frac{1}{2}\cos\alpha \\ 0 & \frac{\sqrt{3}}{2}\cos\alpha & -\frac{\sqrt{3}}{2}\cos\alpha & 0 & \frac{\sqrt{3}}{2}\cos\alpha & -\frac{\sqrt{3}}{2}\cos\alpha \\ \sin\alpha & \sin\alpha & \sin\alpha & \sin\alpha & \sin\alpha & \sin\alpha \\ 0 & -C_{M_\phi} & -C_{M_\phi} & 0 & C_{M_\phi} & C_{M_\phi} \\ 2C_{M_\theta} & C_{M_\theta} & -C_{M_\theta} & -2C_{M_\theta} & -C_{M_\theta} & C_{M_\theta} \\ C_{M_\psi} & -C_{M_\psi} & C_{M_\psi} & -C_{M_\psi} & C_{M_\psi} & -C_{M_\psi} \end{pmatrix} \tag{3}$$

$$u^T = (T_1 \quad T_2 \quad T_3 \quad T_4 \quad T_5 \quad T_6) \tag{4}$$

The matrix A is derived by the arrangement of the rotors. Here, C_{M_ϕ} and C_{M_θ} are

$$C_{M_\phi} = \frac{l}{6}\left(2\sin\alpha + \sqrt{2}\cos\alpha\right) \tag{5}$$

$$C_{M_\theta} = \frac{l}{18}\left(2\sqrt{3}\sin\alpha + \sqrt{6}\cos\alpha\right) \tag{6}$$

The C_{M_ψ} is a constant derived by the relation between the rotational speed and anti-torques of the rotors.

2. 2 Motion Simulation

To evaluate the motion performance of the dot-HR, motion simulation is held. The remarkable point is movement in the horizontal direction

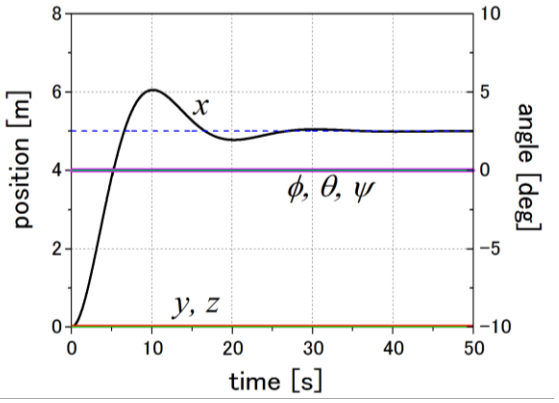

Fig. 3 Simulation result of position and attitude

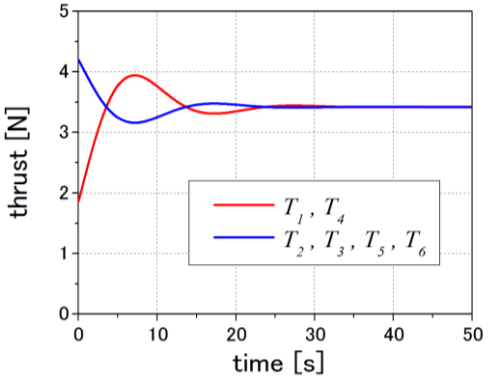

Fig. 4 Simulation result of thrust

without tilting. Figure 3 shows time history of position and attitude moving 5 [m] along *x*-axis. Figure 4 shows the change of thrust in same motion. T_1 to T_6 are thrust of rotor 1 to 6.

It is confirmed that attitude of the dot-HR does not change when the dot-HR moves along *x*-axis by Figure 3. The rotor 1 and 4 add power for acceleration. The rotor 2, 3, 5 and 6 reduce power for acceleration moving along *x*-axis. By the motion simulation, it is also confirmed that the dot-HR is able to fly omnidirectionaly without tilting.

3 Experimental Setup

3. 1 Experimental Testbed

The experimental testbed of the dot-HR is constructed and conducted some tests. Figure 5 shows the experimental prototype of the dot-HR. The experimental testbed is built with the elements shown in Figure 6, which is mainly divided into attitude control system and navigation system.

Fig. 5 Experimental testbed of the dot-HR

For the attitude control, gyro sensor and accelerometer is used with microcomputer to work as Inertial Measurement Unit (IMU) and derives the attitude angle and attitude angular velocity of the vehicle. Attitude angle is basically derived by the integral of the angular velocity measured by the gyro sensor, but the MEMS sensors loaded on the vehicle has high sensing errors against their advantages of being small, lightweight, and low power consumption. The attitude angle derived by the integration accumulates the error as the time passes and differs from the actual attitude angle. Also, the accelerometer is able to measure the attitude angle by using the gravity force with small accumulation but measures the motion and

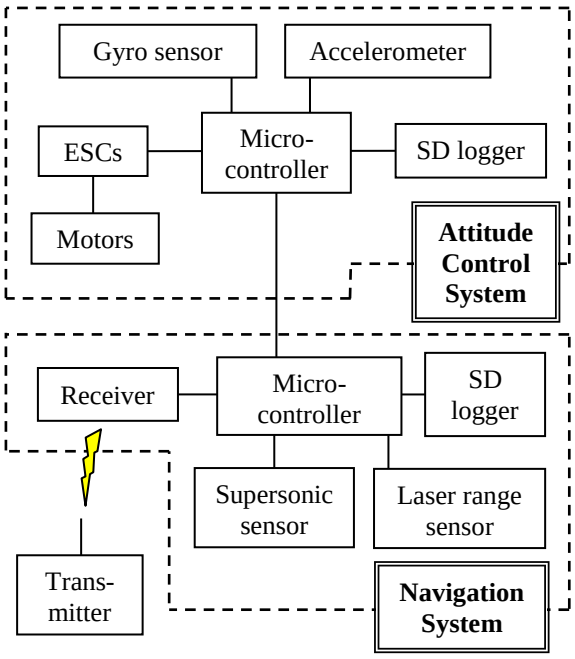

Fig. 6 Summary of the experimental prototype

vibration of the vehicle which makes it hard for the sensor to measure the attitude themselves.

To overcome this problem, the conventional Extended Kalman Filter (EKF) for the IMU is brought in. EKF consists of time update step and measurement update step which calculates both state prediction and covariance of the error at the same time. The covariance is minimized using Kalman gains with predicted and measured states. In this system, the accumulated errors from the gyro sensor will be modified by the accelerometer, so the time update and measurement update are given as the following equations.

Time update

$$\frac{d}{dt}\begin{pmatrix}\phi\\ \theta\end{pmatrix} = \begin{pmatrix}1 & \sin\phi\tan\theta\\ 0 & \cos\phi\end{pmatrix}\begin{pmatrix}p\\ q\end{pmatrix} \tag{7}$$

Measurement update

$$\begin{pmatrix}acc_x\\ acc_y\end{pmatrix} = \begin{pmatrix}g\sin\theta\\ g\sin\phi\end{pmatrix} \tag{8}$$

In this experiment, ϕ and θ are the only states that are used in control, so Euler equation (8) does not consist ψ in the equation.

To stabilize the vehicle, Linear Quadric Regulator (LQR) is brought in to design the control system. Equation (9) shows the state equation for attitude of the rotorcraft.

$$\frac{d}{dt}\begin{pmatrix}\phi\\ \theta\\ \psi\\ \dot{\phi}\\ \dot{\theta}\\ \dot{\psi}\end{pmatrix} = \begin{pmatrix}0&0&1&0&0\\ 0&0&0&1&0\\ 0&0&0&0&1\\ 0&0&0&0&0\\ 0&0&0&0&0\\ 0&0&0&0&0\end{pmatrix}\begin{pmatrix}\phi\\ \theta\\ \psi\\ \dot{\phi}\\ \dot{\theta}\\ \dot{\psi}\end{pmatrix} + \begin{pmatrix}0&0&0&0&0&0\\ 0&0&0&0&0&0\\ 0&0&0&0&0&0\\ 0&-C_{\ddot{\phi}}&-C_{\ddot{\phi}}&0&C_{\ddot{\phi}}&C_{\ddot{\phi}}\\ 2C_{\ddot{\theta}}&C_{\ddot{\theta}}&-C_{\ddot{\theta}}&-2C_{\ddot{\theta}}&-C_{\ddot{\theta}}&C_{\ddot{\theta}}\\ C_{\ddot{\psi}}&-C_{\ddot{\psi}}&C_{\ddot{\psi}}&-C_{\ddot{\psi}}&C_{\ddot{\psi}}&-C_{\ddot{\psi}}\end{pmatrix}\begin{pmatrix}T_1\\ T_2\\ T_3\\ T_4\\ T_5\\ T_6\end{pmatrix} \tag{9}$$

Here, $C_{\ddot{\phi}}$, $C_{\ddot{\theta}}$ and $C_{\ddot{\psi}}$ are

$$C_{\ddot{\phi}} = \frac{C_{M_\phi}}{I_x} \tag{10}$$

$$C_{\ddot{\theta}} = \frac{C_{M_\theta}}{I_y} \tag{11}$$

$$C_{\ddot{\psi}} = \frac{C_{M_\psi}}{I_z} \tag{12}$$

Here, the gain matrix Q for the state variables in LQR is as shown in equation (13). q_{11}, q_{22} corresponds to attitude angle ϕ and θ in equation (9), and q_{33}, q_{44}, q_{55} corresponds to angular velocities p, q, r.

$$Q = \begin{pmatrix}q_{11}&0&0&0&0\\ 0&q_{22}&0&0&0\\ 0&0&q_{33}&0&0\\ 0&0&0&q_{44}&0\\ 0&0&0&0&q_{55}\end{pmatrix} \tag{13}$$

The gain matrix R consists of diagonal matrix with r_{11} to r_{66}, but all of the rotors are treated as equal which leads to the matrix R being an Eigen matrix with all the gains as 1.

For the navigation control, ultrasonic sensor and laser range sensor is loaded. The ultrasonic sensor is used to range sensor to measure altitude of the vehicle, and the laser range sensor is used for obtaining the information of the unknown surrounding environment.

3. 2 Experimental Methodology

The sensing system and attitude control system for the vehicle is investigated in this paper. The measurement accuracy of the IMU and attitude stability will be examined. To evaluate the measurement accuracy and attitude stability, the vehicle is constrained on the mount to have 1 degree of freedom around single axis and the thrust for hovering is applied. The result around y-axis is explained in this paper.

Fig. 7 Experimental system of attitude feedback

To evaluate the experimental results properly, the motion of the vehicle is measured by the 3 dimensional motion capture system and the data is used as actual data of the vehicle to be compared with the data obtained by the IMU.

4 Experimental Results

Using the experimental setup, Figure 8 to Figure 17 shows the results of the experiment. Here, the "actual" is the data from 3-dimensional motion capture system.

4. 1 IMU Accuracy Test

Figure 8 is the result of IMU accuracy test for onboard system. In this experiment, the experiment mount for attitude control system is used. The mount is tilted approximately 30 [deg] around y axis, and the data from IMU and actual data are compared.

Figure 9 shows the error between θ_{actual} and θ_{IMU}. The maximum error is relatively big as of 5.73 [deg] but basically in between ± 3 [deg], which we can consider the system as feasible measurement system for the vehicle.

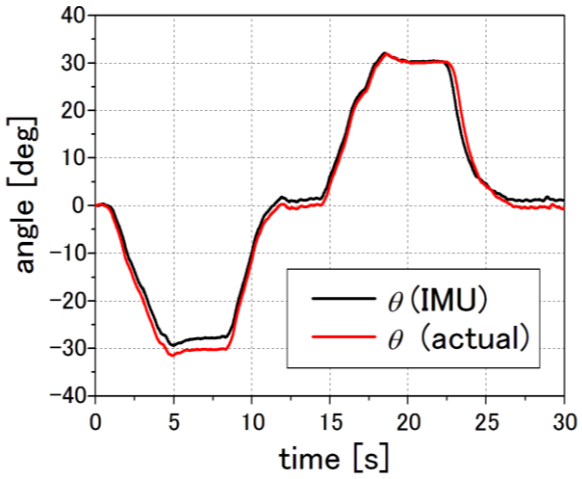

Fig. 8 Result of IMU accuracy testing

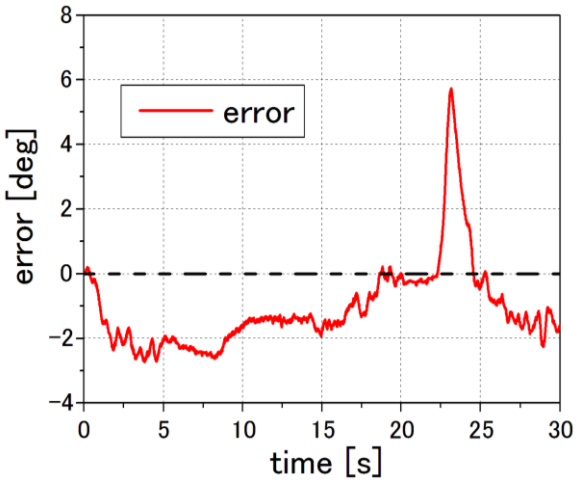

Fig. 9 Error of IMU

4. 2 Attitude Stabilization Control Test

Figure 10~14 shows the time history of attitude angle angular velocity, thrust of the hovering input with the vehicle embedded on the experimental mount in 1 degree of freedom. The parameters for LQR are shown in Table 1. Here, q_{11}, q_{22}, q_{33} and q_{44} are derived from the numerical simulation, and q_{55} for ψ is heuristically chosen from the experiment results.

Figure 10, 11 and 12 show small vibration in attitude angle, angular velocity and thrust, but has stabilized throughout the control without diverging. Figure 13 shows the relation between attitude and thrust of the vehicle. By this figure thrust 3, 4 and 5 adds power, and thrust 1, 2 and 6 reduces power when θ and q are positive. By the Figure 2, it is confirmed that such a thrust control decrease θ and q. The experiment results show that the vehicles attitude is able to be controlled by the LQR. Also, Figure 14 is the close up of figure 10, showing the data after certain duration of time. Compared to the results from IMU accuracy test, the errors due to the disturbance from motor and the others, the error around 20 [s] becomes quite large between the actual value. But after 21 [s], the EKF designed in previous section has updated the sensing data from the accelerometer which modifies the data close to actual value after 22 [s].

Table 1 Parameters of LQR

q_{11}, q_{22}	q_{33}, q_{44}	q_{55}
100	50	1

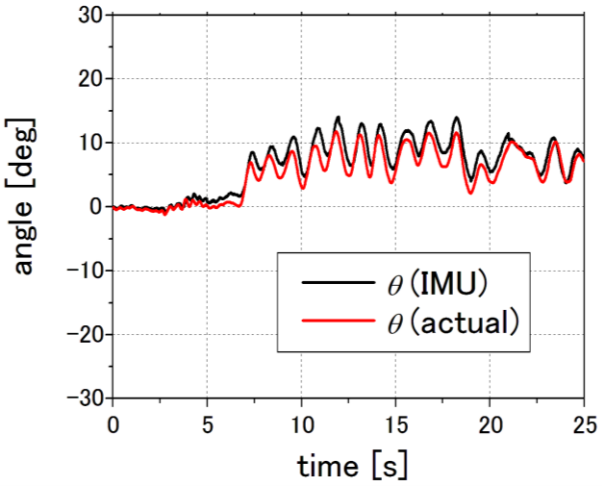

Fig. 10 Stability test result of angle

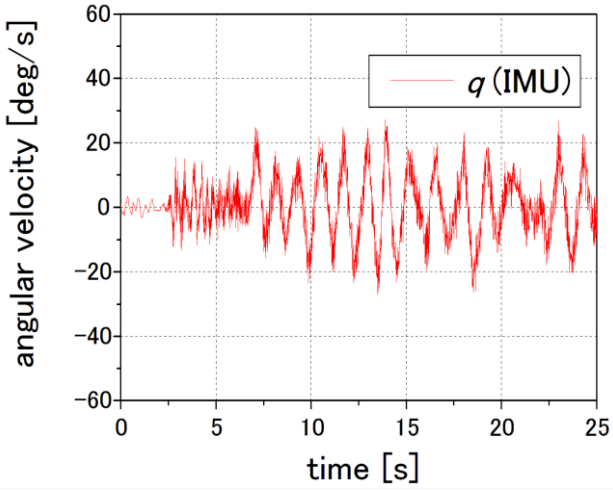

Fig. 11 Stability test result of angular velocity

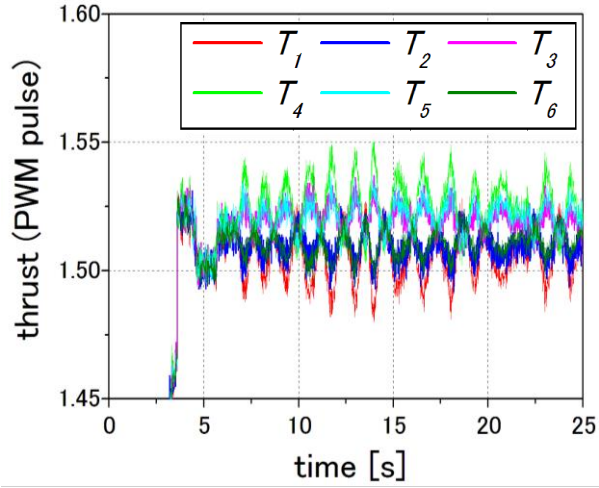

Fig. 12 Stability test result of thrust

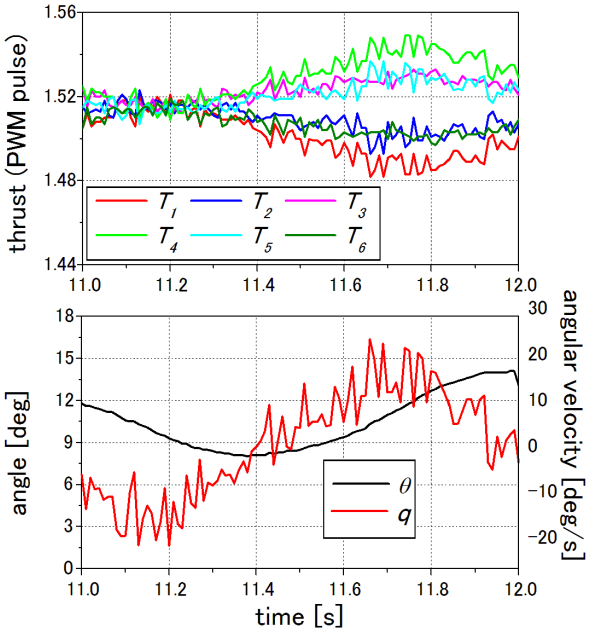

Fig. 13 Stability test result of LQR

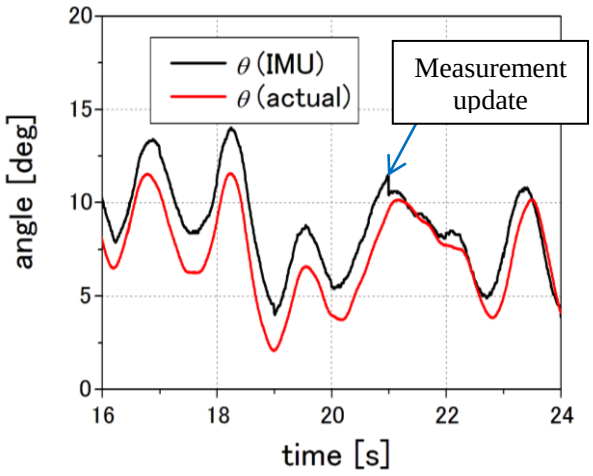

Fig. 14 Measurement update of EKF

4. 3 Free Flight Experiment

Figure 15-17 shows position, attitude angle and angular velocity of the vehicle of indoor free flight experiment. In this experiment, the vehicle is commanded hovering and moving in the horizontal direction without tilting. The attitude of the vehicle is controlled automatically using attitude control system, and the position is controlled with manual operations using transmitter.

In Figure 15, the vehicle starts at the origin and moves in the surge direction. Figure 16 and 17 show small vibration in attitude angle and angular velocity. However,

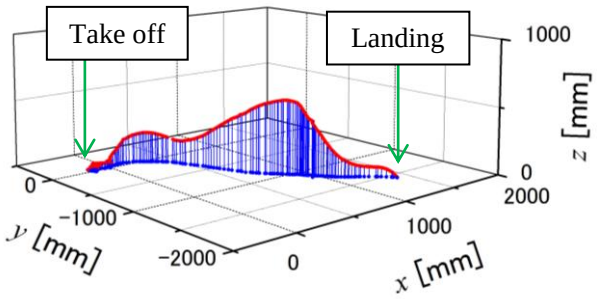

Fig. 15 Free flight result of position

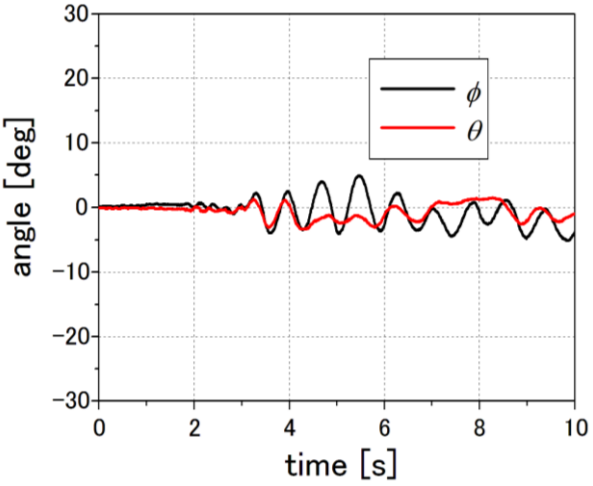

Fig. 16 Free flight result of angle

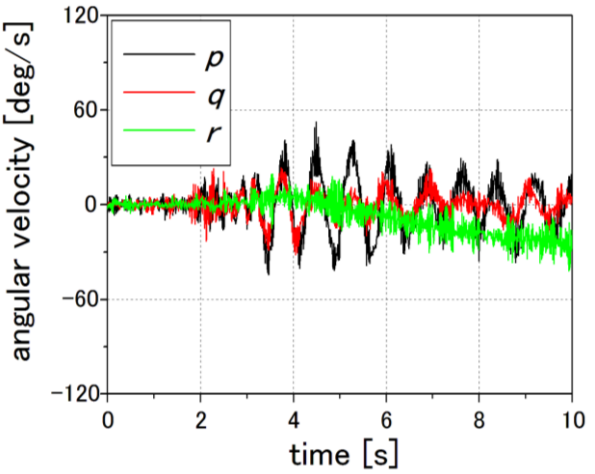

Fig. 17 Free flight result of angular velocity

traditional rotorcrafts need incline more and constant attitude angle when it moves in the horizontal direction. So, it is confirmed that the dot-HR testbed is able to move without tilting its attitude by these results.

5 Conclusion

The double tetrahedron Hexa-Rotorcraft is proposed. Firstly, the motion performance of the dot-HR is confirmed by the numerical simulation. To verify these simulation results, the testbed of the dot-HR is constructed, and tested its elements before free flight.

From the IMU accuracy test, the IMU to be loaded on the new multi-rotor has shown the ability to measure proper attitude of the vehicle. Also, the attitude controller has been designed using the data from IMU and has shown that the vehicle is able to be stabilized in the experiment.

From these results, the free flight experiment is held. In this experiment, the vehicle hovers and moves in the horizontal direction without tilting its attitude. This motion is impossible for traditional rotorcrafts. So, finally, the unique ability of the dot-HR is confirmed.

References

[1] G. Hoffmann et al. The Stanford Testbed of Autonomous Rotorcraft for Multi Agent Control (STARMAC). *Proc. of the 23rd Digital Avionics Systems Conference*, Salt Lake City, UT, 12.E.4, 2004.

[2] N. Guenard et al. Dynamic modeling and intuitive control strategy for an "X4-flyer". *Proc. of the 5th International Conference on Control and Automation*, Budapest, Hungary, Vol. 1, pp 141-146, 2005.

[3] Rahul Goel et al. Modeling, Simulation and Flight Testing of an Autonomous Quadrotor. *Proc. of the 11th Centenary International Conference and Exhibition on Aerospace Engineering*, pp 18-22, 2009.

[4] P. Pounds et al. Design of a Four-Rotor Aerial Robot. *Proc. 2002 Australasian Conference on Robotics and Automation*, Auckland, New Zealand, pp 27-29, 2002.

[5] Mario Valenti et al. Indoor Multi-Vehicle Flight Testbed for Fault Detection, Isolation, and Recovery. *Proc. of AIAA GN&C Conference*, Keystone, Colorado, AIAA 2006-6200, 2006.

[6] Girish Chowdhary et al. Integrated Guidance Navigation and Control for a Fully Autonomous Indoor UAS. *Proc. of AIAA GN&C Conference*, Portland, Oregon, 2011

[7] C. Basnayake et al. Int. Journal of Vehicle

Information and Communication Systems. *An HSGPS, inertial and map-matching integrated portable vehicular navigation system for uninterrupted real-time vehicular navigation*, Vol. 1, Nos. 1/2, pp 131-151, 2005.
[8] Rafael Toledo-Moreo et al. Journal of IEEE Transactions on Intelligent Transportation Systems. *Lane-Level Integrity Provision for Navigation and Map Matching With GNSS, Dead Reckoning, and Enhanced Maps*. Vol. 11, Issue 1, pp 100-112, 2010.
[9] D. M. Sobers et al. Laser-Aided Inertial Navigation for Self-Contained Autonomous Indoor Flight. *Proc. of AIAA GN&C Conference*, AIAA Paper 2010-8211, 2010.
[10] David H. Shim et al. Autonomous Exploration in Unknown Urban Environments for Unmanned Aerial Vehicles. *Proc. of AIAA GN&C Conference*, San Francisco, California, 2005.
[11] Jose Guivant et al. Journal of Robotic Systems. *Autonomous Navigation and Map building Using Laser Range Sensors in Outdoor Applications*, Vol. 17, No. 10, pp 565-583, 2000.
[12] T. Higuchi, K. Kokubu, and S. Ueno. SICE Journal of Control, Measurement, and System Integration. *Experiment of Collision Avoidance Control Law with Information Amount Feedback,* 2012, (Accepted).

Copyright Statement